Arabian Journal for Science and Engineering (2020) 45:4077–4089
https://doi.org/10.1007/s13369-020-04385-x

RESEARCH ARTICLE-CIVIL ENGINEERING

Model Testing on Failure Mechanism of Tunnel Face in Sandy Cobble Stratum

Junwei Zhang[1] · Ling Huang[1] · Taixin Peng[1] · Haoquan Wang[1] · Yichong Zhang[1] · Liang Guo[1]

Received: 1 September 2019 / Accepted: 23 January 2020 / Published online: 13 February 2020

Abstract
One of the universal problems in shield tunneling is face collapse caused by the sudden change of the soil in front of the tunnel face in weak sandy pebble stratum. In order to control the sudden change of the soil, the model test method is used to study the stability of the tunnel face in the sandy pebble stratum. The results indicate that (1) in sandy pebble stratum, the instability mode of the tunnel face can be divided into four stages of slow development stage, transition stage, rapid development stage and instability stage; (2) the influence of the ratio of the soil depth and the support pressure on the instability of the tunnel face can be divided into three stages of the insensitive stage, the sensitive stage and the failure stage; (3)finally, the instability failure shape of the sand–pebble stratum is upward developing in the lower part "chimney shape," while the upperpart of the surface presents "spiral shape" subsidence and ultimately presents "crater shape"; (4) when excavation face is unstable, the surface horizontal settlement groove meets the normal distribution curve proposed by Peck and is similar to the settlement shape measured by the test. The study also found that the bamboo sticks with sand inserted in the soil in front of the tunnel face can increase the friction between the bamboo sticks and compact the soil, make the soil more prone to form soil arches, and effectively control the deformation of the soil in front of the tunnel face.

Keywords Sandy cobble stratum · Shield tunnel face · Similitude principle · Tunnel face failure · Laboratory test · Deformation control

1 Introduction

The rapid development in urban underground infrastructures has resulted in an increased demand for the construction of tunnels in adverse geological conditions such as sandy cobble stratum, which can result in the ground movements, damage existing surface structures, roof fall or face collapse at shallow depths. To control ground displacements, in particular against tunnel face collapse, the shield construction method has been extensively used. However, it is hard to avoid the disturbance of the shield to the surrounding environment and even lead to excessive ground subsidence. Since the end of the 19th century, a large number of scholars have taken the prevention of the instability of the tunnel face as the starting point, analyzed the stability of the tunnel face as the core, determined the minimum support force as the key point, and obtained the relevant solution of the limit support force of the tunnel face by theoretical research [1–3]. The numerical simulation method is used to simulate the instability failure of the tunnel face [4–6]. The indoor test method is used to carry out the stability and instability failure of the shield tunnel face [7–9]. However, considering the complexity of site construction conditions, compared with the theoretical research and numerical simulation analysis, the scale model test can more truly restore the complex engineering and geological conditions in the site, and more convenient to observe the interaction of rock and soil mass. Scholars at home and abroad have conducted a lot of research.

Kamata [10], Chen [11] and Kirsch [12] achieved the purpose of simulating the shield excavation of the tunnel through the retreat of the face plate, so as to simulate the impact on the stability of the tunnel face during the full section excavation. But the simulation of the tunnel excavation by adopting the integral tunnel model retreat lacks the research on the formation loss. Zhu [13, 14] used the self-designed shield tunneling model to get the theory of stratum adaptability between the design principle of shield machine and the phys-

✉ Junwei Zhang
zhangjun_wei@126.com

[1] School of Geosciences and Technology, Southwest Petroleum University, Chengdu 610500, Sichuan, China

ical and mechanical characteristics of stratum. He did not notice that it is necessary to further study the feasibility of combining the actual engineering with the physical experiment through the similitude principle. Similarly, Berthozh [8], Le [15] and Chambonh [16] not only have studied the failure modes of tunnel faces in different soil layers, but also lack of research on sandy pebble stratum.

To sum up, a large number of scholars have studied the stability of tunnel face in different soil layers by physical experiment methods. However, some key experiments problems remained not to be solved: (1) the reduction in the support pressure of the tunnel face leads to the instability of the soil in front of the tunnel face, without considering the cause of stratum loss; (2) combining the actual project with the indoor test, without really considering the shield work participation The adaptability between the number and the physical and mechanical properties of the stratum; (3) the present experiments mostly simulate the single sandy soil layer, silt soil layer, clay soil layer and loess soil layer, and the types of soil layers studied are mostly concentrated on the sandy soil layer and clay soil layer, and the research on sandy pebble soil layer is very little. In order to further improve the scale model test research on the stability of shield tunnel face, this paper, combined with the actual project, determined the main similarity ratio in the model test according to the similarity principle of soil shield system. The material ratio tests were determined according to the similarity relationship between the prototype and the model. The inflated and deflated air bag is used to simulate the working condition of too large and too small supporting force of the tunnel face. The bamboo sticks with sand and pebble particles were taken to reinforce the soil in front of the tunnel face to control the deformation of the soil, so as to study the deformation and instability mode of the tunnel face of the shield tunnel in the sandy pebble stratum.

2 Test Preparation

2.1 Project Overview

The first section of the Chengdu Metro Line No. 18 is located in the Gaoxin area of Chengdu. It is composed of two sections. The first section is South Railway Station—Fuhuayuan Station, and the second section is Fuhuayuan Station–Jincheng Square Station. The tunnel starts at the southern end of the South Railway Station and ends at the northern end of Jincheng Square Station, with a total length of 6085.03 m. The tunnel face stability in sandy cobble stratum is the research object in this paper. ZCK10 + 535.703–ZCK13 + 021.999 is the beginning and the end of the South Railway Station to the Fuhuayuan Station. The left line is 2459.296 m. (The middle wind shaft is 27 m long.) The right line is 2485.897 m. And centerline spacing between both tunnels is 15.89–32.3 m. The covered depth of the tunnel is 8.3–22.9 m. The maximum slope in the shield tunnel is 24%. The minimum curve radius $\boldsymbol{R}$ is 450 m. The maximum excavation diameter is 8.6 m. Geology between the South Railway Station and the Fuhuayuan Station is covered by the Quaternary (**Q**) stratum. And the surface is mostly covered by artificial fill (**Q4ml**). Under the surface is the alluvial (**Q4al**) clay, silty clay, silt, the Upper Pleistocene ice deposit, alluvial (**Q3fgl + al**) pebble soil lenticular sand, and the underlying bedrock are the upper Cretaceous irrigation port (**K2g**) mudstone. And the rock layers traversed by the internal tunnel are mainly medium and dense pebble soil, dense pebble soil and intermediary weathered mudstone, as shown in Table 1.

Table 1 Geological statistics of shield tunnel face

Section	Mileage	Length (m)	Geological section
South Railway Station—Fuhuayuan Station	YDK10 + 535.703–YDK10 + 556.102	19	Middle density sand gravel
	YDK10 + 556.102–YDK10 + 953.762	397.6	The upperpart is pebble soil, and the lower part is intermediary weathered mudstone
	YDK10 + 953.762–YDK13 + 021.999	2068	Weathered mudstone in full section

The terrain at the site is generally flat, with a ground elevation of 490.1–494.953 m. The topography is a grade II terrace of the Fanjiang Plain of the Minjiang River. Depending on the regional geological data, there is no fracture within the scope of the project. The rock formation is a monoclinic structure, and the rock formation is nearly horizontal output. The geological profile of the tunnel entrance is illustrated in Fig. 1.

In this project, the content of pebbles is high: the strata crossing the tunnel are mainly medium and dense pebble soil, dense pebble soil and middle weathered mudstone. The pebble content of the layer is up to 55–70%. The maximum particle size of the pebble is about 180 mm, and about 4–7% of the boulders are locally sandwiched, and the particle size is 210–300 mm.

2.2 Scale Model Test Device and Soil Material Ratio

2.2.1 Test Device

The fully transparent visual steel frame model is used to carry out the tunnel face support pressure test and simulates shield tunnel excavation test, as shown in Fig. 3. The overall model

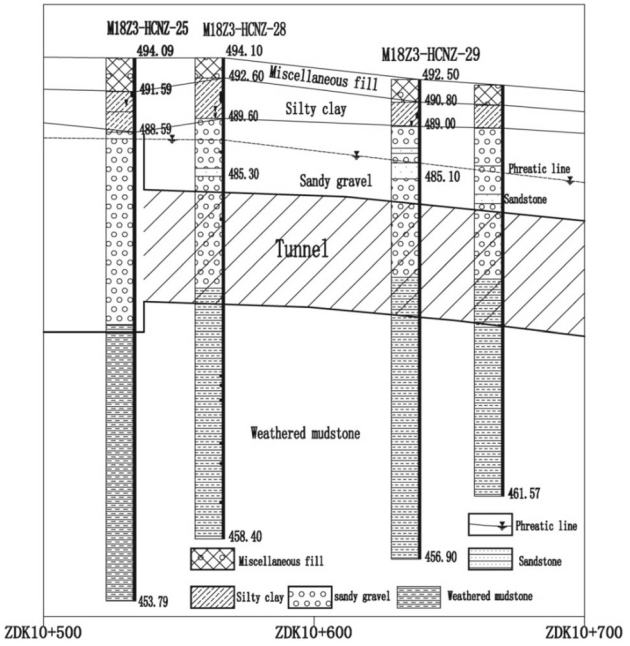

Fig. 1 Schematic geology diagram of tunnel entrance section

size is 0.9 m × 0.9 m × 0.7 m (length × width × height). The plexiglas panel on the full and semicircular shield model presents the longitudinal and cross-sectional instability failure process and sliding zone of the shield tunnel face. The model scale ratio is controlled according to the tunnel aperture. The tunnel aperture of this model is 0.11 m. According to the outer diameter of the shield machine in Chengdu Metro Line 18, the outer diameter of the model is 75 times. The scale model is shown in Fig. 2.

The rubber airbag device is installed in the tunnel model, and the concept of simulated shield tunnel head instability device is shown in Fig. 3. The air compressor is used to pressurize and decompress the airbag to realize the expansion and contraction of the tunnel to simulate the increase and decrease in the retaining surface support force to observe the surface uplift and settlement caused by the shield excavation.

2.2.2 Similitude Theory

The scale model test needs to satisfy the first and second similarity theorems. According to the elastic mechanics problem, the similarity criterion and similarity ratio of model test are deduced. Indoor scale model and field in situ test model should meet the basic equations in speech and action mechanics, such as balance equation, compatibility equation, physical equation, geometric equation, and boundary conditions.

According to theoretical analysis, the physical quantities are as follows: (1) shield characteristics, including cover soil thickness $h(L)$, shield diameter $D(L)$, shield weight $G(L)$; (2) soil properties, including cohesion $c(FL^{-2})$, internal friction angle φ (1), soil bulk density $\gamma(FL^{-3})$, soil deformation modulus $E(FL^{-2})$, Poisson's ratio, μ; (3) dependent variable, including internal stress of soil $\sigma(FL^{-2})$, soil deformation $\delta(L)$, strain ε.

The relation of physical quantities can be expressed by the following equation.

$$f(\sigma, E, \mu, \varphi, \varepsilon, \delta, D, h, G, c, \gamma, l) = 0 \tag{1}$$

There are 12 characteristic parameters in Eq. (1) altogether. The bulk density γ and geometric size l are selected as the basic physical quantities. If $n = 12, m = 2, n - m = 10$, the number of dimensionless factors π is 10. So π_1 is given as

$$\pi_1 = \frac{\sigma}{\gamma^a l^b} = \frac{Fl^{-2}}{(Fl^{-3})^a l^b} \tag{2}$$

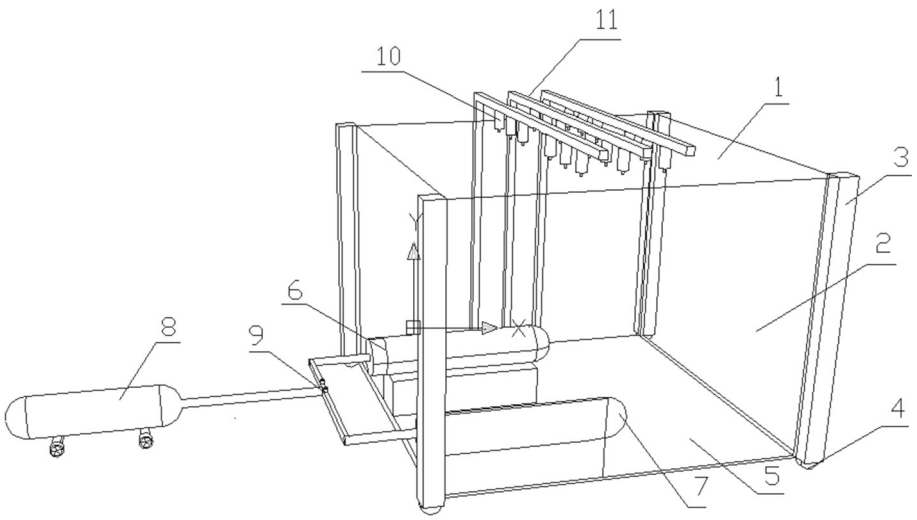

Fig. 2 Schematic diagram of the simulated shield excavation instability test device (1-model box, 2-tempered glass, 3-frame, 4-caster, 5-base, 6-tunnel model, 7-balloon, 8-air compressor, 9-valve, 10-displacement meter, 11-bracket)

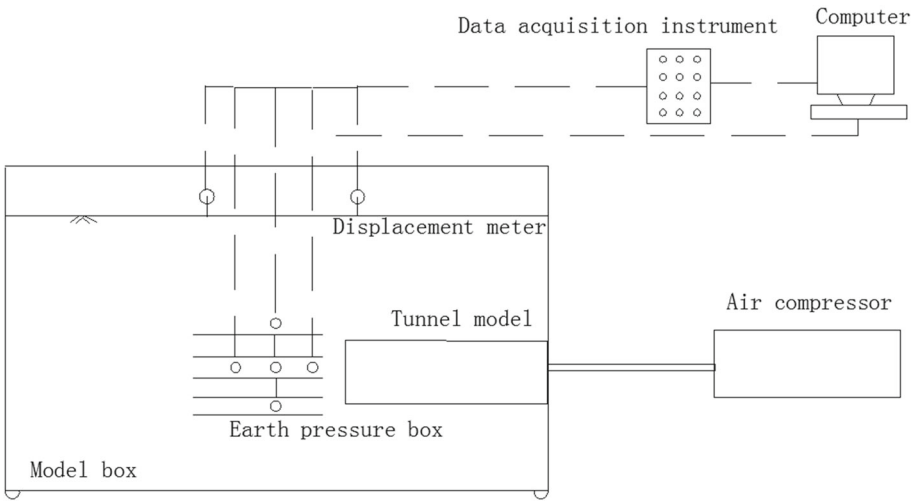

Fig. 3 Conceptual diagram of simulated shield excavation instability test device

Table 2 Similarity ratio parameter of scale model test

Mechanical parameters	Deformation modulus Es/MPa	Internal friction angle φ/°	Poisson's ratio μ	Soil bulk density γ/(kN/m^3)
Soil layer				
Prototype sand pebble	25–50	35–42	0.22–0.23	20–22
Similarity ratio	75:1	1:1	1:1	1:1
Model material	0.30–0.6	35–42	0.22–0.23	20–22

Then, $a = 1, b = 1$. Equation (3) is obtained by Eq. (2).

$$\pi_1 = \frac{\sigma}{\gamma l} \tag{3}$$

Similarly, the following results can be obtained.

$$\pi_2 = \frac{E}{\gamma l}, \pi_3 = \mu, \pi_4 = \varphi, \pi_5 = c, \pi_6 = \varepsilon, \pi_7 = \delta, \pi_8 = D, \pi_9 = h, \pi_{10} = \frac{G}{\gamma l^3}$$

According to the similarity of the two mechanical phenomena, the similarity criterion is obtained:

$$\frac{c_\sigma}{c_\gamma c_l} = 1, \frac{c_E}{c_\gamma c_l} = 1, \frac{c_c}{c_\gamma c_l} = 1, c_\mu = c_\varphi = c_\varepsilon = 1, \frac{c_\delta}{c_l} = \frac{c_D}{c_l} = \frac{c_h}{c_l} = 1, \frac{c_G}{c_\gamma c_l^3} = 1.$$

The relationship π function of the item is:

$$f\left(\frac{\sigma}{\gamma l}, \frac{E}{\gamma l}, \frac{c}{\gamma l}, \frac{\delta}{l}, \frac{D}{l}, \frac{h}{l}, \frac{G}{\gamma l^3}, \mu, \varphi, \varepsilon\right) = 0 \tag{4}$$

where σ is the internal stress of the soil, E is the deformation modulus of the soil, c is the cohesion, μ is the Poisson's ratio, φ is the internal friction angle, ε is the strain, δ is the deformation of the soil, D is the diameter of the shield, h is the thickness of the soil, G is the shield self-weight.

Seventy-five is the scale ratio between the scale test model and the actual engineering in situ size model, that is, the geometric similarity ratio is 75, and the volume-to-weight ratio is 1. According to the above similarity ratio theory, the similarity ratio of other parameters is obtained, as shown in Table 2.

2.2.3 Determination of Model Similar Material

The prototype soil referenced by the model test was taken from the sand–pebble stratum of the tunnel from the South Railway Station to the Global Central Station in Chengdu Metro Line 18. The geometric similarity ratio is determined by the diameter of the prototype shield and the model shield. Diameter similarity ratio of prototype shield and model shield is 75 in Table 1. The diameter of prototype shield machine is 8300 mm, and the diameter of scale shield model is 110 mm. The configuration of the model soil is performed according to the above similar relationship. Stress, elastic modulus, cohesion, and similarity ratio are 75, that is $c_\sigma = c_E = c_c = 75$. The bulk density, Poisson's ratio, internal friction angle, and strain similarity ratio are 1, that is $c_\gamma = c_\mu = c_\varphi = c_\varepsilon = 1$.

According to the engineering geological survey report of the tunnel excavation section of the Chengdu Metro Line 18 tunnel, the physical and mechanical parameters of the sand pebble and the material parameters corresponding to the model are shown in Table 3.

Table 3 Physical and mechanical parameters of engineering sand pebble and material parameters required for scale model test

Parameter	Symbol	Value
Geometric	C_L	75
Bulk weight	C_γ	1
Poisson's ratio	C_μ	1
Strain	C_ε	1
Friction angle	C_φ	1
Strength	C_S	75
Stress	C_σ	75
Cohesion	C_c	75
Elastic model	C_E	75

2.3 Material Ratio Test

The original soil size was reduced according to the geometric similarity ratio of 75 to test. Considering the strong instability of the pebble formation without cementation, loose rock mass, low overall strength of the surrounding rock mass, poor self-stability, it must be taken into account the fact that the friction angle remains constant in the scale model. The proportioning test is mainly composed of small size pebbles, gravel and coarse sand, and mixed with a certain proportion of medium sand and water. The single cycle process mainly includes the following tests: material weighing, drying, soil particle screening test, and direct shear test.

2.3.1 Screening Test

From the soil sample, a certain mass is taken for the particle grading analysis test. In order to understand the overall similarity of the sand grains with different particle sizes, the percentage of particles smaller than a certain particle size to the total mass of the sand will be determined to understand sand composition, analysis of particle size distribution, determination of sand classification and determination of its properties. The particle grading curve is shown in Fig. 4.

The unevenness coefficient C_u and the curvature coefficient C_C are as follows:

$$C_\mathrm{u} = \frac{d_{60}}{d_{10}} = \frac{0.80}{0.01} = 8.0 \tag{5}$$

$$C_\mathrm{C} = \frac{d_{30}^2}{d_{10}d_{60}} = \frac{0.23^2}{0.80 \times 0.01} = 6.61 \tag{6}$$

Classification is carried out according to soil gradation. If $C_\mathrm{u} \geq 5$ and $C_\mathrm{C} = 1$–3, and the sand is well graded, otherwise it can be judged as poor gradation. The natural graded soil sample used in this test is a poor grade of sand according to the calculation results of C_c. It has been verified that the particle gradation curve of the soil sample is consistent with the distribution of the soil sample gradation curve collected by Chengdu Metro Line 18.

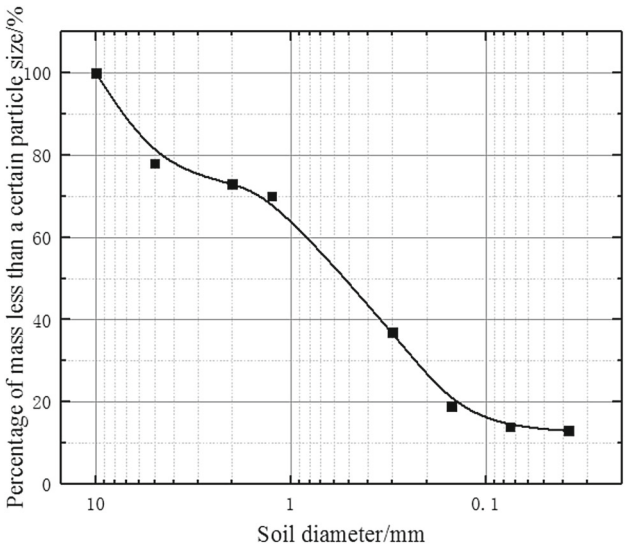

Fig. 4 Particle grading curve

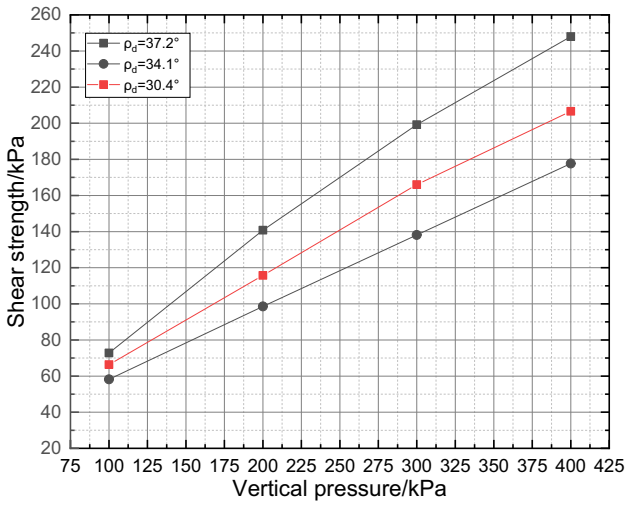

Fig. 5 Relationship between shear strength and vertical pressure at different densities

2.3.2 Direct Shear Test

The dry density of loose sand pebbles by laboratory tests is about 1.9 g/cm^3. The dry density of slightly dense sand pebbles is about 2.0 g/cm^3. And the dry density of dense sand pebbles is about 2.1 g/cm^3. Direct shear test was carried out on three different densities of sand and gravel samples (dry density: $\rho_\mathrm{d} = 1.9$ g/cm^3, 2.0 g/cm^3, 2.1 g/cm^3). The test results are shown in Fig. 5.

According to the buried depth of sand pebbles of Chengdu metro line 18 is 8–12 m, the thickness is 14–20 mm, mainly

Table 4 Model sand pebble soil material ratio

Stratum	Pebble	Gravel	Coarse sand	Nakasuna	Water
Size/mm	4–8	2–4	0.5–2	<0.5	
Sand pebble	1	0.41	1.94	1.16	0.64

sub round pebbles, a small amount of round pebbles, the content is 50–85%, the content of 20–200 mm pebbles is about 50–70%, the particle size is generally 20–80%, the content of boulders of 210–300 mm is generally 4–7%, the filler is mainly medium coarse sand and fine sand, the similar theory is combined with screening test and direct shear test to model test materials. The material proportion of model sand pebble is shown in Table 4.

3 Model Test Design

3.1 Purpose of the Test

Combining with field measurement, the stability of the tunnel face in sandy pebble stratum is studied by a model test. To provide reliable analytical basis for practical engineering, the specific research contents are as follows.

1. Full and semicircular shield tunnel model are used to observe the longitudinal and transverse failure process and sliding zone of the shield tunnel face through the plexiglass panel. The failure process, failure shape, deformation, settling crate ahead of tunnel face need be studied, respectively, before the failure mechanism of shield tunnel face is determined.
2. Using the earth pressure box on the shield support panel, the distribution characteristics of earth pressure before shield excavation are studied. Supporting pressure is too large will cause surface uplift, and supporting pressure is too small will lead to surfacing collapse, which will cause the change of earth pressure in front of excavation. Therefore, it is necessary to study the support pressure of shield tunneling along the tunnel face on the mechanism of tunnel face instability.
3. Shield tunneling is a very complex construction process, so it is necessary to study the influencing factors of stability of shield tunnel face. This test mainly studies the influence of different buried depth, i.e., $C/D = 0.5$, 1.0, 2.0 and 3.0, on the stability of shield tunnel face in the case of different density of sand pebble: slightly dense, medium dense and dense, and soil property.

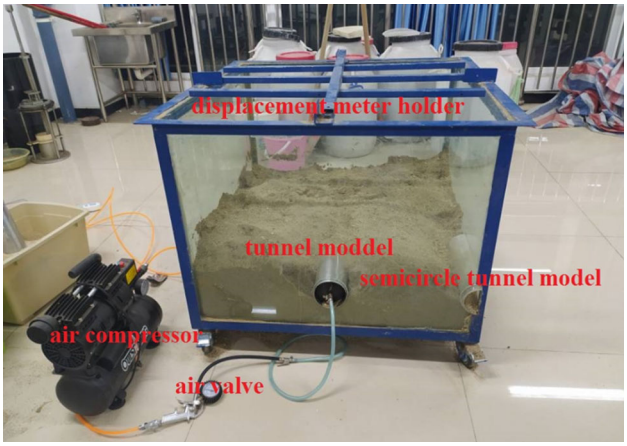

Fig. 6 Field test diagram of simulated shield excavation instability test device

3.2 Test Device

A shield tunneling test device and method for simulating stratum settlement is provided aiming at the problem that the stability of shield tunnel face is difficult to control. It can simulate the instability of the tunnel face and the collapse of the stratum caused by too small support force. The failure mechanism is revealed by monitoring the support force of the tunnel face and the displacement of the soil. The concrete model is shown in Fig. 6.

The test device comprises a model box, a tunnel model, an air compression device, a monitoring system and a data processing system. The model box size is 900 mm × 900 mm × 700 mm (long × width × height), surrounded by fully transparent tempered glass. The model box frame is made of steel plate, and the bottom of the model box is provided with casters and can be moved and fixed. The model box is provided with a basis for placing the tunnel model. The model box is provided with a full circular hole and a semicircular hole on the front side of the model, which can be used for the shape of the sliding area of the horizontal and vertical sections simultaneously observed, and the full circular hole and the semicircular hole are used for placing the tunnel model, and the tunnel model is made of stainless steel.

For the increase and decrease in the support pressure, the air bag and air compressor are used to simulate. The air bag is placed inside the tunnel model to simulate the support force of the tunnel face, and the air compressor is used to supply the gas inside. The air compressor can provide 30 L of high-capacity air pressure, enough to provide sufficient air pressure for the airbag. The air compressor is equipped with a pressure gauge, which can accurately display the air compressor air pressure value, and the air valve control between the air compressor and the airbag. The process of balloon expansion and contraction is shown in Fig. 7.

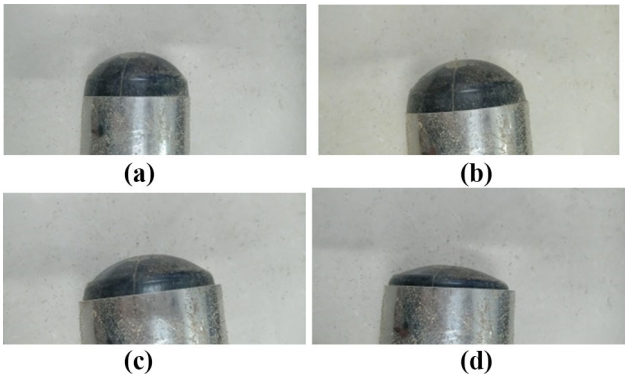

Fig. 7 Change graph of the stage of air bag expansion and contraction

The monitoring system includes a displacement gauge and a soil pressure box. The displacement gauge is used to monitor the displacement of the soil. The earth pressure box is used to monitor the change of the earth pressure on the tunnel face. The displacement measuring range is 30 mm, and the displacement change of less than 0.005 mm can be resolved. The displacement meter is fixed on the top bracket of the soil layer by using a 100% magnetic base, and the earth pressure box has a range of 30 kPa. The displacement meter is connected by a side outlet. And the processing system includes a data acquisition device for acquiring the monitoring system, the data acquisition device is coupled to a processing device for storing and analyzing morphological parameters, and the processing device outputs processing data. The data acquisition device is configured to acquire the settlement amount measured by the displacement meter and the earth pressure change amount monitored by the earth pressure box, and the data acquisition device and the strain gauge are connected to the processing device, wherein the processing device is a computer system.

3.3 Test Procedure

The model test device can be used to simulate ground settlement and uplift caused by tunnel face instability. The main steps are as follows:

(1) Prepare the sample soil according to the actual working conditions.
(2) Place the sample soil into the model box to the model slot position.
(3) Install the tunnel model, arrange the earth pressure box in the soil in front of the tunnel face, continue to add soil to the position required for the test, and arrange the displacement meter on the top of the soil.
(4) Connect the displacement meter and the earth pressure box to the data acquisition instrument, and prepare the instrument for debugging.
(5) Insert the air bag and connect the air bag to the air compressor.
(6) Take an air compressor to pump the airbag until the required support pressure, record the change of soil displacement and earth pressure.
(7) Repeat the steps (1)–(5), use the air compressor to pump the airbag, and deflate the airbag before the soil is bulged until the soil collapses, and record the soil displacement and the earth pressure.
(8) Repeat steps (1)–(7) until the instability law of the tunnel face is found.

4 Instability Analysis of Tunnel Face

4.1 Instability Mode Analysis of Tunnel Face

When the support force provided by the airbag changes, the deformation and destruction shape of the tunnel face are also different. Generally, the stability of the tunnel face can be reflected by the support pressure ratio. Therefore, reducing the support force of the airbag in the test simulated to release the stress of the surrounding rock, the instability process of the tunnel face is observed.

In order to compare with the static earth pressure, the support pressure ratio λ is introduced, given as

$$\lambda = \frac{\sigma_s}{\sigma_0}$$

where σ_s is the support pressure of the tunnel face, and σ_0 is the horizontal static earth pressure at the center of the shield.

When the support pressure changes, the transverse section, longitudinal section and surface deformation of the tunnel face are shown in Figs. 8, 9 and 10. The smaller the support pressure ratio is, the larger the disturbance range of the tunnel face is $\lambda = 0.62$, $\lambda = 0.43$, $\lambda = 0.18$ and $\lambda = 0.12$ represent four stages of tunnel face instability development, respectively. Seen from Fig. 8, soil subsidence near the tunnel face shows a U-shaped trend with very large openings when $\lambda = 0.62$, and the angle of collapse shape (assuming that the tangent of the slip surface formed in the soil is at an angle to the horizontal plane) is very small at the first stage of tunnel face instability. And it is shown in Fig. 9 that the influence area of soil develops upward, which is roughly elliptical, and the surface is not loosened from the overlook in Fig. 10. The soil ahead of the tunnel face has been disturbed from the center point of the airbag. This is consistent with the position where the air bag initially reduces air pressure. Because the action range of soil arch effect is not obvious, the deformation of soil-losing ahead of the tunnel face is slow and appears a downward trend. But there is no obvious downward displacement.

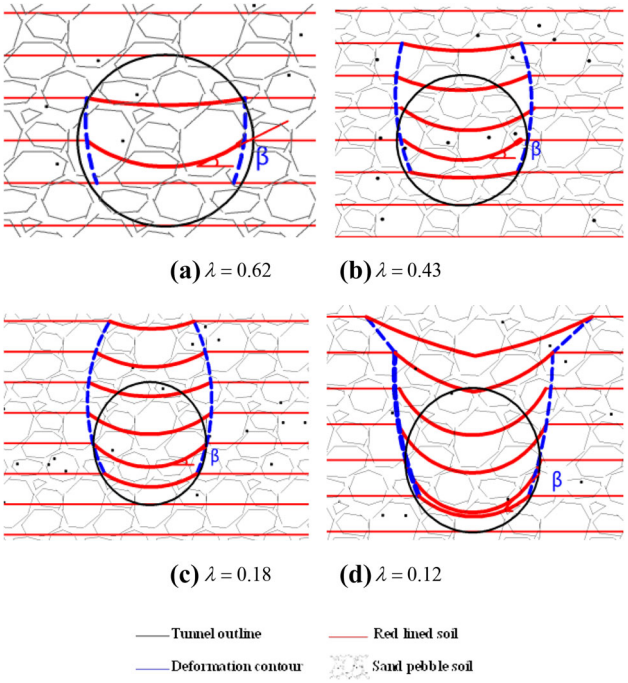

Fig. 8 Sketch of the transverse section deformation of the tunnel face with different support pressure ratios at $C/D = 0.5$

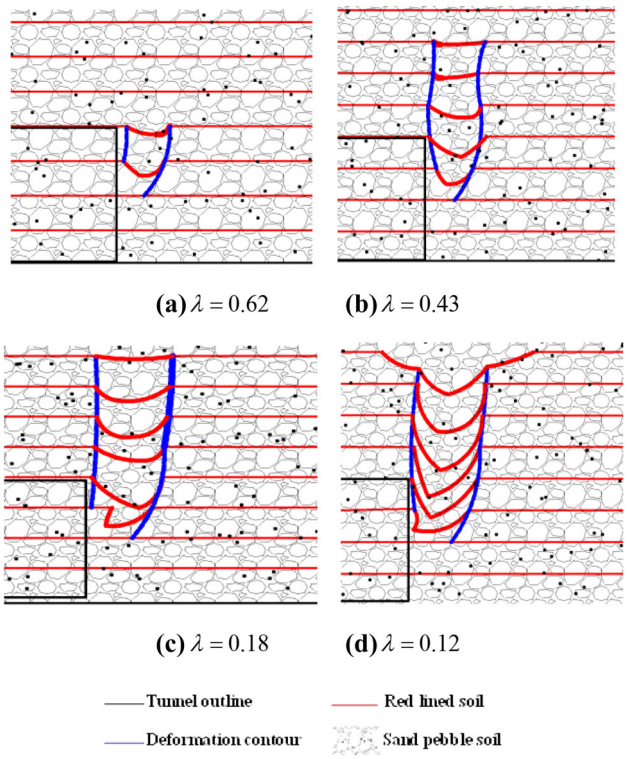

Fig. 9 Sketch of longitudinal section deformation of tunnel face with different support pressure ratio at $C/D = 0.5$

When $\lambda = 0.43$ at the second stage of tunnel face instability, the soil arch area near the tunnel working face develops

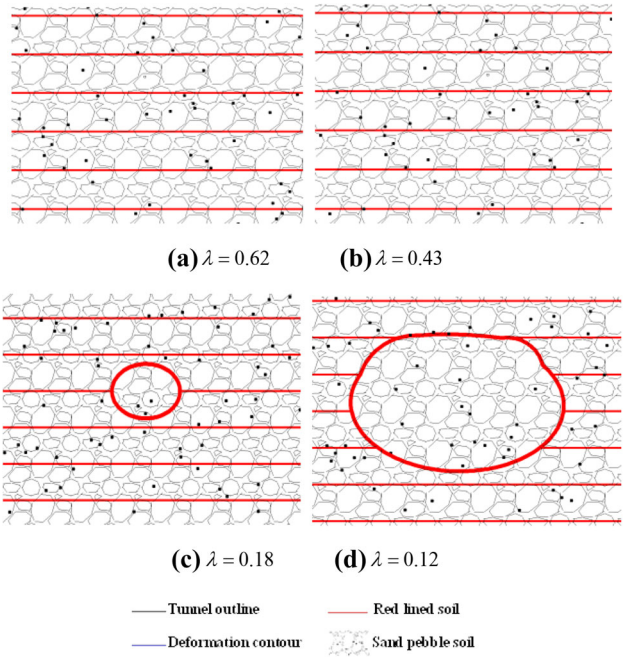

Fig. 10 Schematic sketch of the tunnel face of different support pressure ratios at $C/D = 0.5$

upward, and the angle of collapse shape β becomes larger gradually, as shown in Fig. 8. From the longitudinal section in Fig. 9, the soil failure presents a long ellipse shape and has a deformation tendency to expand, while from the overlook, the soil does not deform in Fig. 10. It can be also seen from Fig. 8 that the scope of soil loosening is larger than that of $\lambda = 0.62$, and the damage scope of the surrounding rock of the vault begins to develop upward at the tunnel face. This phenomenon is more obvious in Fig. 9 when it has not yet spread to the surface.

At the third stage of tunnel face instability, that is $\lambda = 0.18$, the instability of the tunnel face is accelerating. And the loosening range continues to expand (Fig. 8). The soil arching effect disappears when the failure range of the tunnel face spreads to the surface. At this time, the surface displacement begins to increase. From the transverse section in Fig. 8, the U-shaped opening at the beginning of the vault position becomes smaller, and the angle β of collapse shape continues to increase. From the vertical section in Fig. 9, the soil deformation expands to the surface, while from the top view in Fig. 10, the surface change is elliptical.

$\lambda = 0.12$ is the fourth stage of the tunnel face instability. The soil in front of the tunnel face collapses slowly until it reaches maximum surface deformation. Collapse shape of the bottom soil is still U-shaped, but the angle becomes larger, the soil is squeezed together, and there is no obvious demarcation line. The shape of the collapse surface is basically formed from the position of the vault. At the bottom of the collapse

shape, a sharp angle appears which is conical. From the transverse section in Fig. 8, the bottom of the collapse shape of the vault appears sharp angle, which is valley-shaped. From the longitudinal section in Fig. 9, the collapse shape angle of the vault collapse shape reaches the maximum, and the whole is V-shaped.

4.2 Failure Shape of Tunnel Face

It is found by the results of centrifugal experiments on the stability of the tunnel face in the early years of simulating clay stratum shield tunneling that the tunnel face failure modes in sand and viscous soil layers are different [17] as shown in Fig. 11. It shows that the failure shape of the tunnel face in the sand layer is characterized by the chimney-like upward development. In the cohesive soil layer, due to the cohesive force between the soil particles, the failure surface is characterized by a basin with a lower portion. At the same time, it is pointed out that the minimum support pressure that satisfies the stability of the tunnel face has little effect when the covered depth is constant.

By comparing the damage shape diagram of the failure mechanism of the tunnel face in sand and viscous ground layer, as shown in Fig. 12, it can be found that this experiment results are slightly different from the fracture pattern of the tunnel face in different soil layers given by Mair et al [17]. The specific performance is that when the damage surface of the tunnel face has not yet reached the surface, and the shape of the longitudinal section of the tunnel face is "chimney-like" upward. And in the event of ultimate destruction, the shape of the damage reaching the surface is "valley-like," and the bottom of the surface subsidence has sharp corners. But it is not the chimney damage of the sand layer that has been studied by Mair et al [17]. The shape is such that the lower part is a large "U-shaped broken shape," and the upperpart is a "V-shaped" with a large opening, and it is not a simple deformed surface studied by Mair et al.

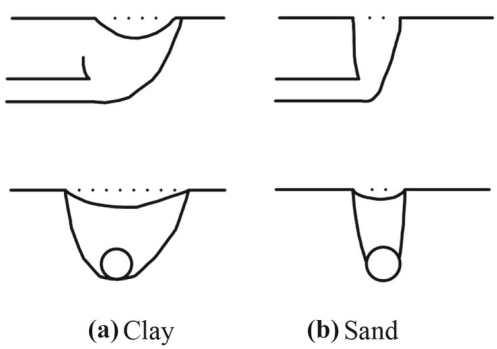

Fig. 11 Destruction shape of different soil layers [17]

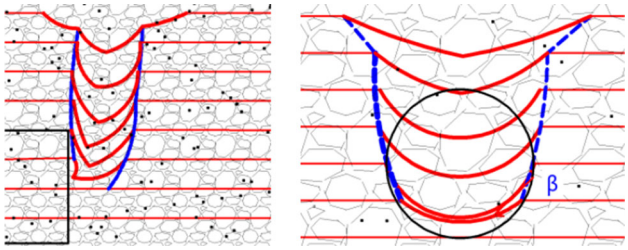

Fig. 12 Sketch of the completely destroyed shape of the tunnel face of the sand–pebble stratum

4.3 Surface Deformation

In the test, the support force of the tunnel face was reduced by controlling the air pressure in the airbag at a constant speed, and the instability of the tunnel face was observed. When the instability deformation of the tunnel face reaches the third stage, the process of surface subsidence to complete collapse can be observed, as shown in Fig. 13. The support pressure ratio is gradually reduced from (a) to (d) in Fig. 14. Although the ratio decreases slightly, the collapse process is very rapid. The first collapse area formed by surface deformation and subsidence is elliptical, and the failure range increases with the decrease in support pressure ratio, the subsidence area increases rapidly. When a certain location is reached, the area of subsidence will not increase, but the surface subsidence will increase. The final settlement shape is spiral subsidence, and there are settlement steps.

Surface subsidence failure of tunnel face under different working conditions is observed in this experiment. As shown in Fig. 14, the ratio of buried depth in figure (a)–(d) increases in turn. From the test results, it can be observed that: (1) with the increase in buried depth ratio, the area of subsidence decreases, but the shape of subsidence is ellipse at last; and (2) when the buried depth ratio is $C/D = 0.5$, the collapse is very large. When the buried depth ratio is increased to $C/D = 1$, the collapse is still obvious. But when the buried depth ratio is increased to $C/D = 2$, the settlement is obviously weakened. When the buried depth ratio is increased to $C/D = 3$, there is almost no settlement on the surface, indicating that the increase in the buried depth ratio reaches a certain value and does not affect the surface deformation.

4.4 Surface Settlement Crater Fitting

As shown in Figs. 15, 16 and 17, when the support pressure is too small, the measured surface settlement trough is in good agreement with the Peck curve and corresponds well with the measured surface settlement value, which shows that the test accuracy is well controlled. When the surface compaction degree increases, the value of surface subsidence decreases, but the change is not significant. When the covered depth

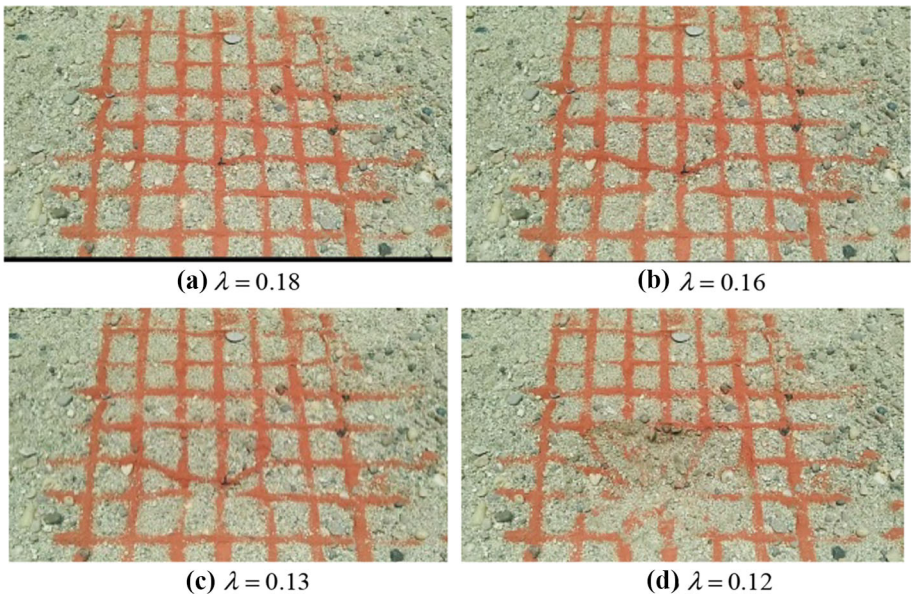

Fig. 13 Surface deformation map of different support pressure ratios at $C/D = 0.5$

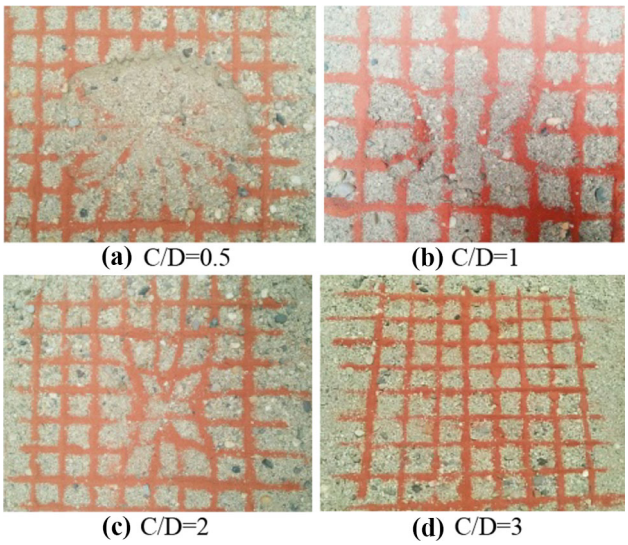

Fig. 14 Surface deformation map of different depth ratios

increases, the surface subsidence decreases, and the change value is larger than that when the soil compactness changes, but when the covered depth ratio increases to a certain extent, it no longer affects the surface subsidence, the ground compactness still affects the surface subsidence.

4.5 Tunnel Face Deformation Control

The settlement observed in the test is expected to strengthen the stability of the tunnel face during shield tunnel excavation and control the deformation of the tunnel face. Therefore, advance reinforcement is adopted to pre-reinforce the soil in front of the excavation. The front bolt is used to pre-reinforce the face of the face, so as to achieve the stability of the face of the face, so as to reduce the deformation response of the soil in front of the face of the face caused by excavation, extrusion expansion deformation and pre-convergence deformation, and to control the ground settlement and surface settlement displacement. At the same time, the stress state on the face of the face is improved and the tensile stress near the face of the face is made. Conversion to compressive stress makes full use of the longitudinal arch effect in front of the face, which greatly reduces the plastic zone caused by excavation of weak surrounding rock and further enhances the self-stability of surrounding rock. In the test, the method of simulated support is shown in Fig. 18. Bamboo sticks are used to adhere to sand and pebbles. Bamboo sticks are arranged before excavation to reinforce the soil in front of excavation according to work conditions.

The results of controlling the deformation strength by inserting bamboo sticks into the formation are shown in Table 5. When a small amount of bamboo sticks is added, the soil settlement is reduced, but the change value is not large. With the increase in the number of bamboo sticks, the decrease value of soil settlement becomes larger. Increasing the number of bamboo sticks to a certain amount can effectively reduce the surface subsidence. Bamboo sticks are used to control soil deformation, so that the mechanical effect of soil ahead of tunnel face can be changed from an unstable state to a relatively stable state, thus the tunnel face will be in a relatively stable environment. The sticky sandy pebbles on bamboo sticks will increase the friction of soil, increase the skeleton effect between particles, increase the restraint effect between particles, and make it easier to form soil arching to support the soil. Multiple bamboo sticks will form a group of bamboo sticks, which can squeeze the soil in front of the tunnel face, make the soil in front of the tunnel face be

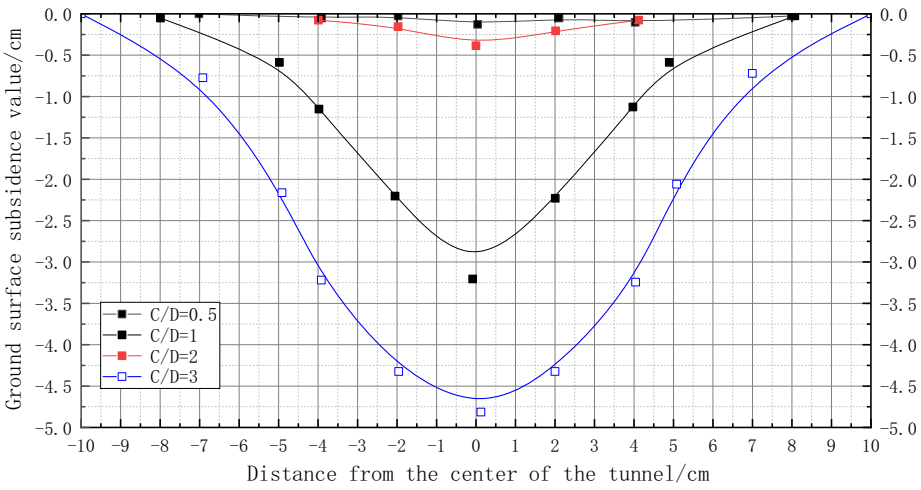

Fig. 15 Surface settlement curves of different covered depths in loose state

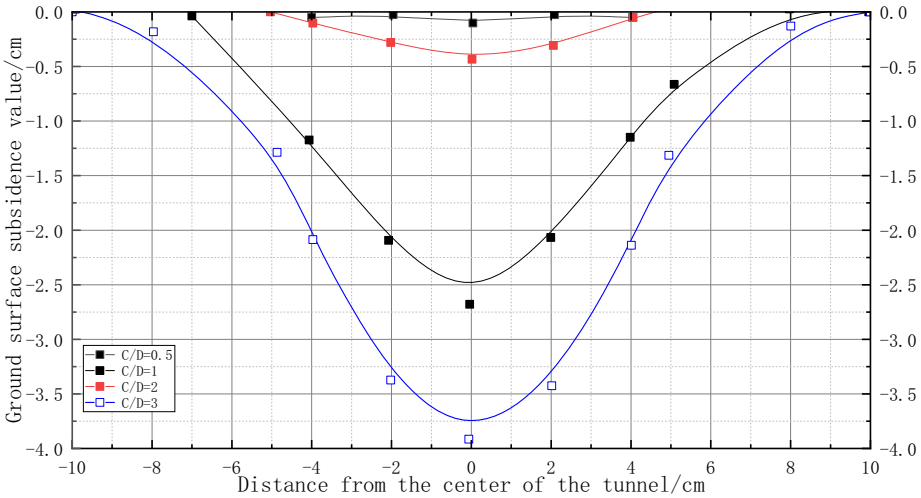

Fig. 16 Surface settlement curves of different covered depths in a slightly dense state

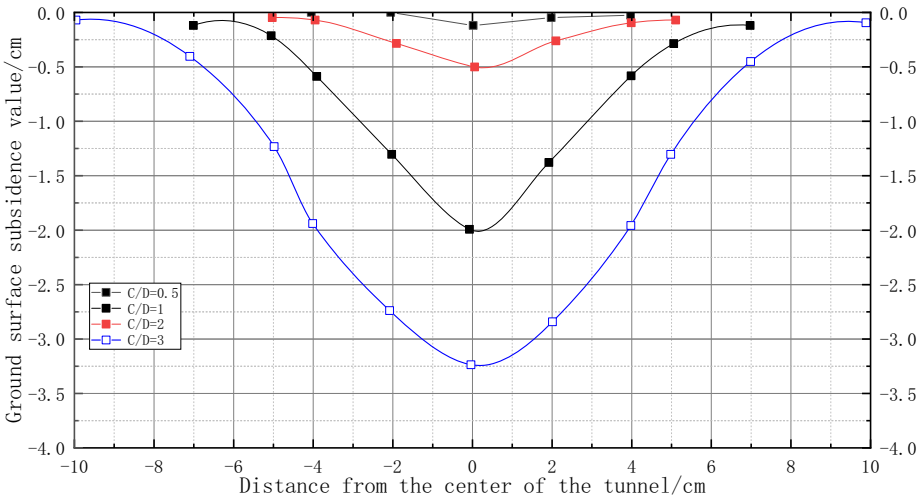

Fig. 17 Surface settlement curves of different covered depths in dense state

Fig. 18 Bamboo stick support diagram

Table 5 Relationship between the number of bamboo sticks and the final settlement value

Number of bamboo sticks/root	0	17	33	50	65	70
Final settlement value/cm	4.8	4.1	2.6	2.0	0.5	0.4

reinforced, also can compact loose sand and pebble particles, better reinforce the soil, enhance the bearing capacity of the soil in front of the excavation.

5 Conclusion

In order to study the deformation and failure of shield tunnel face in sandy gravel stratum, the similarity theory is used to link the model test with the prediction of actual working conditions. A section of the fire hatching shield section of Chengdu Metro Line 18 is selected as the engineering background, and the scale ratio of the indoor test model for the support pressure of tunnel face is determined, and the soil in the model is also determined. The material (pebbles with small size, medium and coarse sand, fine sand and so on) was tested in the laboratory. The expansion and contraction characteristics of air bags are used to simulate the increase and decrease in the support pressure on the tunnel face, so the physical simulation test of shield tunnel in the excavation of sandy pebble is carried out, and the deformation of the tunnel face is also controlled in the case of large settlement value of the tunnel face of sandy pebble. The main contents are as follows:

1. In the sand–pebble stratum, the instability mode of the tunnel face soil can be divided into four stages: slow development stage, excessive stage, rapid development stage and instability stage. When the support pressure is reduced, the soil is disturbed and begins to slowly settle. Due to the soil arching, the soil loses slowly to the surface, causing the surface to settle. When the local surface appears to settle, the soil in front of the tunnel face is quickly instability until the final destruction.
2. The influence of soil depth ratio and support pressure on the stability of tunnel face can be divided into insensitive stage, sensitive stage and failure stage. When the depth ratio increases to a certain extent, it is no longer sensitive to the instability of tunnel face, but when the support pressure ratio of tunnel face is too small, it is no longer sensitive to the instability of tunnel face.
3. The final failure shape of sandy gravel stratum is that when the failure area of tunnel face has not reached the surface, the longitudinal failure profile of tunnel face develops upward in the form of "chimney." When the final failure occurs, the failure shape at the surface is "valley-shaped," and the bottom of the surface subsidence appears sharp angle. The failure cross section of tunnel face is characterized by large "U-shaped failure" at the bottom and large "V-shaped" opening at the top.
4. The relationship between the different buried depth ratio and the horizontal displacement of the soil mass and the surface settlement is parabola. When the support pressure ratio γ is too small, the horizontal settlement groove of the surface meets the normal distribution curve proposed by Peck. At the same time, the vertical settlement curve of the surface also has a similar shape, which is similar to the settlement shape measured by the test. The minimum settlement is on the surface, and the maximum settlement occurs in the tunnel vault.
5. Bamboo sticks with sand and pebble particles in front of shield tunnel excavation can effectively reduce the settlement value caused by soil deformation and instability in front of excavation. This is because bamboo sticks with sand pebbles can increase the friction between loose sand pebble particles, the bamboo sticks used in groups can squeeze the soil more easily to produce soil arch, and restrain the deformation of the soil before excavation, so that the soil before excavation is in a relatively stable state, and then effectively control deformation of shield tunnel face.

Acknowledgements This paper was supported by Basic Applied Research Projects of Sichuan Science and Technology Department, No. 2019YJ0349, C1 Team of Underground Space Development and Utilization, No. X151563, and Natural Science Foundation of China (Nos. 41702340, 41602290).

References

1. Broms, B.B.; Bennermark, H.: Stability of clay at vertical openings. J. Soil Mech. Found. Div. ASCE **96**(1), 71–94 (1967)
2. Broere, W.: Tunnel Face Stability and New CPT Applications. Delft University, Delft (2001)
3. Comejo, L.: Instability at the face: its repercussions for tunneling technology. Tunn. Tunn. **21**, 69–74 (1989)

4. Hernández, Y.Z.; Farfán, A.D.; de Assis, A.P.: Three-dimensional analysis of tunnel face stability of shallow tunnels. Tunn. Undergr. Sp. Technol. **92**, 103062 (2019)
5. Kavvadas, M.; Litsas, D.; Vazaios, I.; Fortsakis, P.: Development of a 3D finite element model for shield EPB tunneling. Tunn. Undergr. Sp. Technol. **65**, 22–34 (2017)
6. Paternesi, A.; Schweiger, H.F.; Scarpelli, G.: Numerical analyses of stability and deformation behavior of reinforced and unreinforced tunnel faces. Comput. Geotech. **88**, 256–266 (2017)
7. Lü, X.; Zhou, Y.; Huang, M.; Zeng, S.: Experimental study of the face stability of shield tunnel in sands under seepage condition. Tunn. Undergr. Sp. Technol. **74**, 195–205 (2018)
8. Berthoz, N.; Branque, D.; Wong, H.; Subrin, D.: TBM soft ground interaction: experimental study on a 1 g reduced-scale EPBS model. Tunn. Undergr. Sp. Technol. **72**, 189–209 (2018)
9. Min, F.; Zhu, W.; Lin, C.; Guo, X.: Opening the excavation chamber of the large-diameter size slurry shield: a case study in Nanjing Yangtze River Tunnel in China. Tunn. Undergr. Sp. Technol. **46**, 18–27 (2015)
10. Kamata, H.; Mashimo, H.: Centrifuge model test of tunnel face reinforcement by bolting. Tunn. Undergr. Sp. Technol. **18**(2), 205–212 (2003)
11. Chen, R.; Li, J.; Kong, L.; Tang, L.: Experimental study on face instability of shield tunnel in sand. Tunn. Undergr. Sp. Technol. **33**, 12–21 (2013)
12. Kirsch, A.: Experimental investigation of the face stability of shallow tunnels in sand. Acta Geotech. **5**(1), 43–62 (2010)
13. Zhu, H.H.; Xu, Q.W.; Fu, D.M.; et al.: Study on design principle of shield machine applicable to differerent strata. Rock Soil Mech. **27**(9), 1437–1441 (2006)
14. Xu, Q.W.; Zhu, H.H.; Fu, S.M.; et al.: Design on model test of tunnel excavation with EPB shield machine in sand stratum. Chin. J. Undergr. Sp. Eng. **2**(3), 361–364 (2006)
15. Le, B.T.; Taylor, R.N.: Response of clay soil to three-dimensional tunneling simulation in centrifuge models. Soils Found. **58**, 808–818 (2018)
16. Chambon, P.; Corté, J.: Shallow tunnels in cohesionless soil: stability of tunnel face. J. Geotech. Eng. **120**(7), 1148–1165 (1994)
17. Mair, R.J.; Taylor, R.N.: Theme lecture: bored tunneling in the urban environment. In: Proceedings of the Fourteenth International Conference on Soil Mechanics and Foundation Engineering, Rotterdam, pp. 2353–2385 (1997)